Development and Optimization of a P-selectin-Functionalized Microfluidic Platform for Modeling Adhesion Dynamics of Ovarian Cancer Cells

Introduction

Background Information:

Ovarian cancer, occurring when cells in the epithelial or other tissues of the ovary undergo uncontrolled division and form a tumor, remains one of the most lethal gynecological cancers among women (An and Yang, 2021; Mazidimoradi et al., 2022). Despite advancements in medicine, ovarian cancer remains challenging to treat due to its high tendency to metastasize and significant recurrence rates. Many studies have highlighted the critical role of metastasis, spreading of tumor cells from the primary tumor to secondary sites, for the progression of ovarian cancer, particularly through peritoneal dissemination. As a result, peritoneal metastasis forms the main route of metastasis for ovarian cancer (Wolters-Eisfeld and Oliveira-Ferrer, 2024). Therefore, characterizing the mechanisms of metastasis, particularly peritoneal metastasis, is fundamental to understanding disease progression.

Selectins are a family of calcium-dependent glycoproteins that mediate cell–cell interactions under shear stress through recognition of specific carbohydrate ligands. Among the selectin family, P-selectin has been implicated in the interaction between ovarian cancer cells and the peritoneal mesothelium. Tumor cells can exploit selectin–glycan interactions to initiate cell tethering and rolling under shear stress, which subsequently facilitates firm adhesion. Sialyl Lewis X (sLe^x) is a recognized carbohydrate determinant involved in P-selectin binding, and its expression has been associated with the metastatic potential of ovarian cancer cells (Hassan et al., 2020). In particular, highly metastatic cancer stem/tumor initiating cells (M-CSCs) exhibit increased sLe^x expression and preferential binding to P-selectin compared with non-metastatic populations. In a previous study from our laboratory, Li et al. identified sLe^x-bearing insulin-like growth factor-1 receptor (IGF-1R) as a major P-selectin-binding determinant on M-CSCs, providing a molecular basis for their enhanced adhesion to the peritoneal mesothelium as illustrated in *Figure 1* (Li et al., 2019).

In their study, Li et al. further demonstrated that the sialyl Lewis X (sLe^x)-P-selectin cascade mediates tumor–mesothelial adhesion under ascitic fluid shear flow. Given that ascitic fluid flows at a very low velocity compared to circulating blood, it was previously assumed that a static microenvironment could be sufficient to support tumor–mesothelial adhesion. However, Li et al. demonstrated that sLe^x–P-selectin-mediated binding occurs under ascitic fluid shear stress rather than under static conditions (Li et al., 2019).

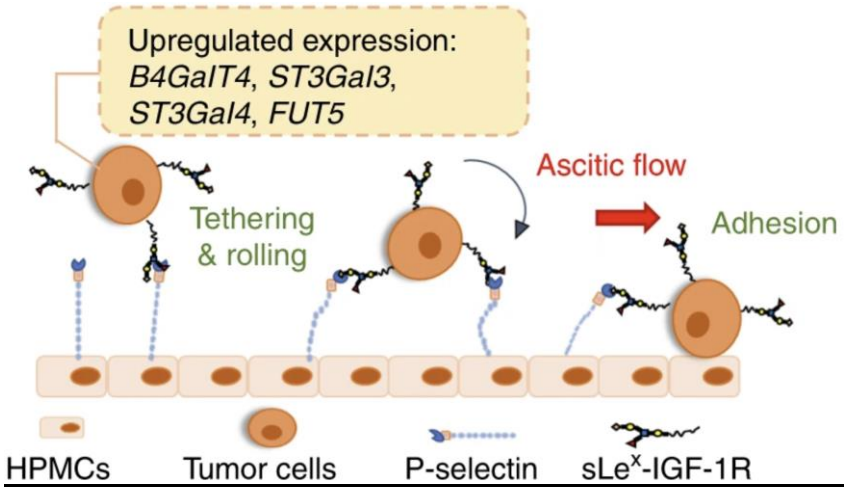

Figure 1. Schematic of sLe^x-P-selectin binding in peritoneal metastasis. HPMCs is an abbreviation for human peritoneal mesothelial cells. Reproduced from Li et al. (2019).

Building on their findings, it is essential to develop sensitive and reliable models of ovarian cancer that account for shear stress conditions to improve our understanding of the mechanisms underlying tumor–mesothelial adhesion. Various in vitro systems have been used to investigate ovarian cancer progression, including conventional static culture, three-dimensional (3D) spheroid models, transwell-based assays, and other flow-based platforms. Although these models provide valuable insights into ovarian cancer biology, they differ in their ability to recapitulate the complexity of the tumor microenvironment. To illustrate, conventional static and three-dimensional models do not adequately reproduce the dynamic mechanical conditions experienced by tumor cells in the peritoneal cavity, including fluid flow and shear stress. Flow-based systems can incorporate these mechanical cues; however, differences in device geometry and flow configuration may affect the distribution and magnitude of shear stress, highlighting the importance of precise control of flow conditions (Cortesi et al., 2024; Smit et al., 2023).

Microfluidics has therefore emerged as a promising tool for studying the effects of fluid flow on cellular behavior. With defined channel geometry and controlled perfusion, microfluidic platforms enable precise manipulation of flow conditions while requiring relatively low sample volumes (Hassan et al., 2020).

Previous work from our group demonstrated that a customizable microfluidic platform could reproduce physiologically relevant shear stress in the peritoneal environment and revealed shear stress-dependent changes in ovarian cancer cell phenotypes (Ip et al., 2016). Subsequently, Li et al. developed this approach to investigate tumor–mesothelial adhesion under ascitic fluid shear flow and demonstrated preferential adhesion of highly metastatic cancer stem cells (M-CSCs) to the peritoneal mesothelium.

Building on these findings, there is a need for optimized microfluidic platforms that can reliably model ovarian cancer cell adhesion under physiologically relevant flow conditions Consequently, this study aimed to investigate and optimize the P-selectin coating concentration for the adhesion of highly metastatic (HM) ovarian cancer cells under microfluidic flow conditions and to compare the sensitivity and specificity of the optimized microfluidic platform using HM and non-metastatic (NM) ovarian cancer cell lines.

Based on previously reported differences in metastatic and functional phenotypes, Kuramochi was selected as the HM cell line, while OVSAHO, OVCAR3, and CaOV3 were selected as NM cell lines for the present study. Previous characterization of HGSOC cell lines demonstrated substantial differences in migration, invasion, proliferation, clonogenicity, and EMT phenotype, with Kuramochi exhibiting relatively high aggressive activity, whereas OVSAHO demonstrated comparatively low functional activity (Haley et al., 2016). More recent molecular and phenotypic profiling has further demonstrated substantial heterogeneity among HGSOC cell lines, including differences in cell morphology, cell-cell adhesion, transcriptional profiles, and EMT-associated gene expression (Piki et al., 2024). In addition, Kuramochi, OVSAHO, OVCAR3, and CaOV3 have been characterized as "peritoneal metastasis of high-grade serous ovarian cancer (HGSOC)" relevant cell-line models (Elias et al., 2015). In vivo studies have also demonstrated differences in tumor formation and metastatic behavior among these HGSOC cell lines, further supporting the use of distinct cell lines to represent different ovarian cancer phenotypes (Mitra et al., 2015). Therefore, these cell lines were selected to investigate differences in P-selectin-mediated adhesion between HM and NM ovarian cancer cell phenotypes under microfluidic flow conditions.

Objectives:

- Determine the optimal working concentration of P-selectin for studying the adhesion of HM and NM ovarian cancer cells under microfluidic flow conditions.
- Compare the sensitivity and specificity of the optimized P-selectin-functionalized microfluidic platform using HM and NM ovarian cancer cell lines.

Methodology

The initial objective was to determine the optimal working concentration of P-selectin for studying the adhesion of HM ovarian cancer cells under microfluidic flow conditions. The subsequent objective was to compare the sensitivity and specificity of the microfluidic chip assays for different HM and NM cell lines. Initially, ten different P-selectin concentrations ranging from 0 to 40 ng/µL were evaluated based on signal intensity and variance. P-selectin concentrations of 25 and 37.5 µg/mL were subsequently selected for downstream optimization experiments. Air bubbles in the microfluidic chip channels were avoided throughout the whole procedure.

1. Microfluidic Chip Preparation and Protein A Coating

Each microfluidic channel was washed twice with 1 mL ethanol, followed by two washes with 1 mL 1× phosphate-buffered saline (PBS). The channels were emptied following the second PBS wash. Protein A was prepared by diluting the 5 mg/mL stock solution 250-fold in 1× PBS to obtain a final concentration of 20 µg/mL. A volume of 60 µL Protein A solution was introduced into each channel, and the chip was incubated for 1 h at room temperature. Following incubation, each channel was washed three times with 300 µL 1× PBS and subsequently blocked with 100 µL 3% BSA for 30 min at room temperature.

2. P-Selectin Concentration Optimization

Initially, ten different P-selectin concentrations ranging from 0µg/mL to 40µg/mL were prepared from a 0.8 mg/mL stock solution by dilution in 1× PBS. Signal intensity and variance were evaluated for these ten different P-selectin concentrations, with results given in *Figure 3* in the Results section.

According to these results, P-selectin concentrations of 25 and 37.5 µg/mL were selected to be used for downstream experiments of the optimization assay (refer to the Results section for rationale for concentration selection).

3. P-Selectin Coating

60 µL of the corresponding P-selectin solution (25 and 37.5 µg/mL) was added to each four channels in microfluidic chips. The chip was incubated overnight at 4°C in a moist chamber. To satisfy the optimal overnight incubation conditions, the moist chamber was prepared using a 120-mm Petri dish, in which a tissue moistened with Milli-Q water was placed under the microfluidic chip. Both ends of each channel were kept moist with Milli-Q water to prevent drying and exposure of the channels to air. The Petri dish was sealed with parafilm to maintain a humidified environment throughout the incubation period.

4. Preparation of the Coated Microfluidic Chip

On the following day, each channel was washed three times with 300 µL binding buffer consisting of 1× PBS supplemented with 1 mM $CaCl_2$ at pH 6.5. Each channel was subsequently blocked with 200 µL blocking solution containing 3% BSA, PBS, 10% FBS, 1 mM $CaCl_2$, and 1 mM $MgCl_2$ and incubated for 30 min at room temperature. Following incubation, the channels were washed three times with 300 µL binding buffer. The chip was then connected to the flow system using microtubing, with one side of each channel connected to the LongerPump and a 200-µL micropipette tip attached to the opposite side. Binding buffer was added to the micropipette tips to maintain hydration of the channels prior to cell loading.

5. HM and NM Cell Preparation

Kuramochi (HM) and OVSAHO (NM) cells were detached from the culture flask using EDTA and collected by centrifugation at 1,000 rpm for 5 min. Following centrifugation, the supernatants were removed and the cell pellets were resuspended to a final concentration of 10^4 cells/ml. An equivalent

volume of the cell suspension was transferred to a corresponding well of a 96-well plate to provide a reference for the initial cell number corresponding to each microfluidic channel.

6. Microfluidic Flow Assay

The prepared HM and NM cell suspensions were introduced into each microfluidic channel by injecting the cell suspension via a syringe into the 200-µL micropipette tip connected to the inlet end of each channel, as illustrated in *Figure 2*. The microfluidic chip was operated using the LongerPump in withdrawal mode, with the flow rate set to 1,500 µL/h and the pump speed set to 425 mm/min, where the outlet is connected to the pump. Cells were subjected to flow for 20 min. During the flow period, the binding buffer level in the 200-µL micropipette tips at the inlet ends was monitored continuously. Binding buffer was replenished as required via a syringe to prevent the introduction of air bubbles into the microfluidic channels and to maintain channel hydration throughout the 20-min flow period.

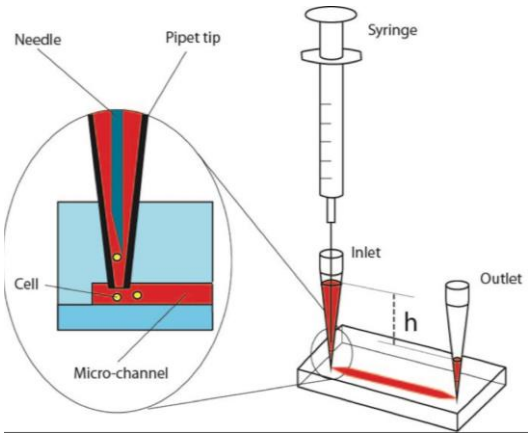

Figure 2. Schematic of cell loading procedure in a microfluidic chip channel. Reproduced from Sadeghi and Elitas (2017).

7. Fluorescence Imaging and Cell Counting

Following staining, fluorescence images were acquired from each individual microfluidic channel using a fluorescence microscope at FITC and TRITC wavelengths. Images were also acquired from the corresponding four wells of the 96-well plate. The number of cells within each microfluidic channel was quantified using QuPath, while the corresponding 96-well samples were used to determine the initial cell number.

8. Calculation of Cell Adhesion

The percentage of cells retained within each channel following the flow assay was calculated as:

Attached cells (%) = (Number of cells remaining in channel after flow) / (Initial number of cells) × 100

The calculated percentage of attached cells was recorded for each P-selectin concentration.

9. Sensitivity and Specificity Analysis

Sensitivity refers to the ability of the microfluidic assay to correctly identify HM cells, whereas specificity refers to the ability of the assay to correctly identify NM cells. Sensitivity and specificity were calculated using the following formulas:

$$\text{Sensitivity (\%)} = TP / (TP + FN) \times 100$$

$$\text{Specificity (\%)} = TN / (TN + FP) \times 100$$

In these formulas, TP (true positive) represents HM Kuramochi cells that were correctly identified as HM based on their adhesion to the P-selectin-coated microfluidic chip. FN (false negative) represents HM Kuramochi cells that were incorrectly identified as NM based on their adhesion response. TN (true negative) represents NM cells (OVSAHO, OVCAR3, and CaOV3) that were correctly identified as NM

based on their lower adhesion to the P-selectin-coated microfluidic chip. FP (false positive) represents NM cells that were incorrectly identified as HM based on their adhesion to the P-selectin-coated microfluidic chip.

Based on the sensitivity and specificity analysis for 25µg/mL and 37.5µg/mL concentrations of P-selectin for (HM) Kuramochi and (NM) OVSAHO cells (*Figure 4A*), 25µg/mL P-selectin concentration was selected for downstream experiments in OVCAR3 and CaOV3 NM cells. For these downstream experiments, steps 1 and 3-8 were repeated for OVCAR3 and CaOV3 (NM) and Kuramochi (HM) cells by using 25µg/mL P-selectin concentration.

10. Data analysis

The percentage of attached cells was compared between HM Kuramochi and NM OVSAHO, OVCAR3, and CaOV3 cells. Graphs were plotted using GraphPad Prism/. Sensitivity and specificity were calculated based on the adhesion responses of the HM and NM cell lines. The 25 µg/mL P-selectin concentration was used for the comparative HM/NM assays following optimization.

Results

P-Selectin Concentration Optimization

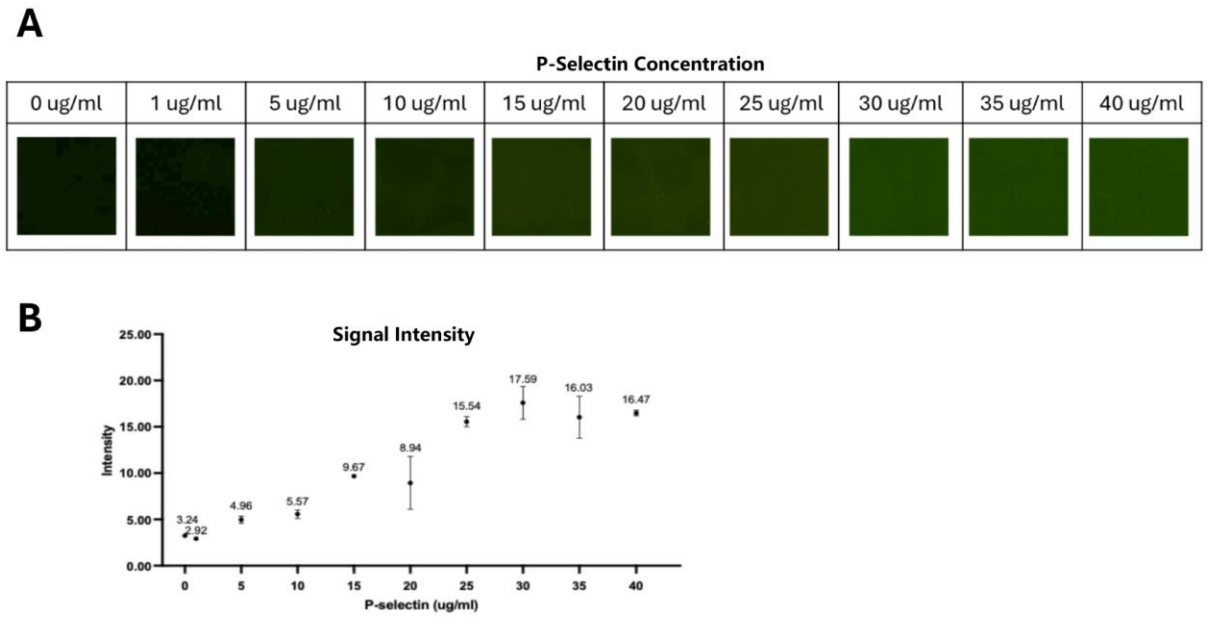

Figure 3. Results for P-selectin concentration optimization assays. ug/ml in the figures represents "µg/mL." Created using GraphPad Prism. Data was provided by Dr. Katie Sze Wai FUNG.
A. Fluorescence results for ten different P-selectin concentrations ranging from 0µg/mL to 40µg/mL.
B. Graph of intensity versus P-selectin concentration for fluorescence signal intensity analysis for ten different P-selectin concentrations used in A.

Based on the signal intensity results, the P-selectin concentration (µg/mL) selected for downstream experiments was 25 µg/mL. As seen in *Figure 3*, 25 µg/mL produced an acceptable signal intensity (15.00) with very low relative variance. Considering the signal intensity and variance, 37.5 µg/mL P-selectin was selected as an alternative to 25 µg/mL to compare their specificity and sensitivity in HM (Kuramochi) and NM (OVSAHO) cells.

Sensitivity and Specificity Analysis

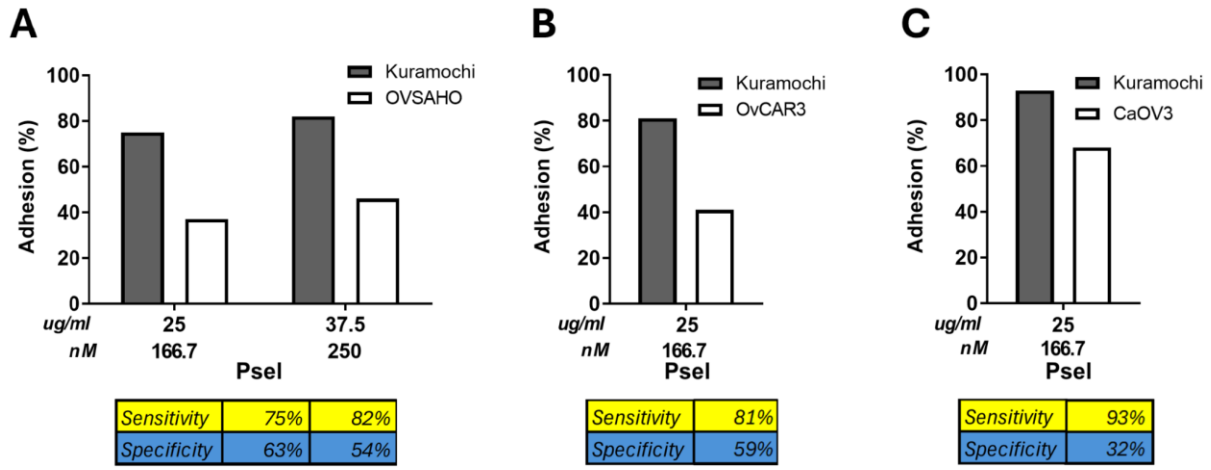

Figure 4. Boxplots for the HM cell line (Kuramochi) and NM cell lines (OVSAHO, OVCAR3, and CaOV3), with the corresponding sensitivity and specificity values shown below each plot. ug/ml in the figures represents "µg/mL." Created using GraphPad Prism. Data was provided by Dr. Katie Sze Wai FUNG.

Microfluidic chip experiments were initially done by using Kuramochi as HM cell line and OVSAHO as NM cell line, with two P-selectin concentrations selected in the upstream experiments as illustrated in *Figure 4A*. The 25 µg/mL P-selectin concentration produced a sensitivity of 75% and a specificity of 63%, whereas the 37.5 µg/mL P-selectin concentration produced a relatively higher sensitivity of 82% and a lower specificity of 54%. Although the 37.5 µg/mL concentration provided higher sensitivity, the 25 µg/mL concentration provided comparatively higher specificity while maintaining an acceptable level of sensitivity (75%). Therefore, the 25 µg/mL P-selectin concentration was selected for downstream experiments using HM (Kuramochi) and NM (OVCAR3 and CaOV3) cell lines.

Following selection of the 25 µg/mL P-selectin concentration, the adhesion responses of HM Kuramochi cells were compared with those of NM OVSAHO, OVCAR3, and CaOV3 cells. The highest sensitivity (93%) was achieved for the Kuramochi and CaOV3 HM/NM pair, while this pair also had the lowest specificity (32%). Similarly, for the Kuramochi and OVSAHO HM/NM pair, the highest specificity (63%) but the lowest sensitivity (75%) was observed (*refer to the Discussion section for the interpretation of reported variation in specificity and sensitivity*).

Discussion

The present study aimed to investigate and optimize the P-selectin coating concentration for studying ovarian cancer cell adhesion under microfluidic flow conditions and to compare the sensitivity and specificity of the microfluidic chip assays for HM and NM ovarian cancer cell lines. Based on the signal intensity and variance results, 25 µg/mL P-selectin was selected for downstream experiments. Comparison of 25 and 37.5 µg/mL P-selectin using HM Kuramochi and NM OVSAHO cells further demonstrated that 25 µg/mL provided a more appropriate sensitivity and specificity profile and was therefore selected for subsequent experiments using OVCAR3 and CaOV3 NM cells. The use of an optimized coating concentration may improve the reproducibility of P-selectin-mediated adhesion measurements and provide a more consistent platform for subsequent investigation of ovarian cancer cell adhesion under flow. Such a platform may be applied to investigate differences in adhesion phenotypes between ovarian cancer cell lines, evaluate P-selectin-mediated tumor-mesothelial interactions, and provide a controlled in vitro model for studying mechanisms associated with ovarian cancer peritoneal metastasis.

In 2019, Li et al. demonstrated that the sialyl Lewis X-P-selectin cascade mediated tumor-mesothelial adhesion under ascitic fluid shear flow and reported preferential adhesion of highly metastatic cancer stem cells compared with non-metastatic cancer stem cells. In the present study, HM Kuramochi cells demonstrated higher adhesion than the NM cell lines, resulting in higher sensitivity but lower specificity for the P-selectin-functionalized microfluidic platform. The observed differences in adhesion between HM and NM cells are consistent with the proposed role of P-selectin-mediated interactions in ovarian cancer dissemination. Therefore, these findings support the use of P-selectin-mediated adhesion as a model for investigating differences in metastatic adhesion phenotypes under flow conditions, since the optimized platform can detect the strong adhesion phenotype of HM cells.

However, the lower specificity observed across the NM cell lines indicates that P-selectin-mediated adhesion may not be sufficiently selective to distinguish all non-metastatic cell lines, and that further optimization is required to improve the ability of the platform to distinguish HM from NM ovarian cancer cells. Optimizing both sensitivity and specificity is therefore crucial for ensuring that the assay can detect HM adhesion responses while minimizing the misclassification of NM cell lines as HM. A balance between these parameters may improve the discriminatory capacity and reproducibility of the assay, thereby increasing its usefulness for comparing adhesion phenotypes across ovarian cancer models.

Furthermore, the variation in specificity observed among the NM cell lines may be associated with biological differences between the cell lines. Previous studies have demonstrated that ovarian cancer cell lines differ in the expression of molecules involved in P-selectin-mediated adhesion. In particular, CaOV3 cells have been reported to exhibit relatively high surface expression of CD24 and sialyl Lewis X (CD15s), both of which are associated with P-selectin-mediated adhesion (Carroll et al., 2018). Therefore, the relatively high adhesion observed for CaOV3 in the present study (*Figure 4C*) may reflect differences in P-selectin-binding capacity between ovarian cancer cell lines, as consistent with findings of Carroll et al. (2018), rather than solely differences in the performance of the microfluidic platform.

Similarly, the differences observed between Kuramochi and OVSAHO may also be related to their distinct cellular phenotypes. Although both cell lines are considered representative HGSOC models, previous studies have demonstrated substantial differences in their migration, invasion, proliferation and EMT-associated phenotypes, with Kuramochi exhibiting relatively high aggressive activity and OVSAHO exhibiting comparatively lower functional activity (Haley et al., 2016). As a result, although the cell lines were selected based on previously reported metastatic and functional phenotypes, the observed variation in specificity suggests that metastatic phenotype does not necessarily correspond directly to P-selectin-mediated adhesion.

Various in vitro systems, including conventional static culture, 3D spheroid models, transwell-based assays, and organoid models, have been used to investigate ovarian cancer progression. However, these models differ in their ability to reproduce the dynamic mechanical conditions of the peritoneal microenvironment. More advanced tumour-on-chip systems can incorporate 3D tumour structures, extracellular matrix, stromal and immune components, biochemical gradients, and controlled mechanical cues, providing greater microenvironmental complexity than the present platform (Lim et al., 2025). Nevertheless, the present microfluidic platform provides a relatively simple and controllable approach for specifically investigating cell adhesion under flow, which is particularly relevant because ovarian cancer cell attachment to the mesothelium is influenced by shear stress. Recent work by Morikis et al. (2026) has similarly demonstrated the utility of microfluidic devices for investigating ovarian tumour cell attachment to mesothelial cells under flow (Morikis et al., 2026).

More advanced ovarian cancer models, including organoid and tumor-on-chip systems incorporating extracellular matrix, stromal cells, immune cells, and other components of the tumor microenvironment, may provide greater biological complexity than the present platform. However, these models may also require more complex experimental systems and are not necessarily designed

specifically to investigate P-selectin-mediated adhesion under controlled shear flow. Therefore, the present microfluidic platform provides a relatively simple and controllable model for studying ovarian cancer cell adhesion under physiologically relevant flow conditions. This may be particularly useful for experiments that focus on adhesion mechanisms, where a simpler platform allows the effects of specific adhesion molecules, such as P-selectin, and different cell phenotypes to be investigated under controlled flow conditions.

Limitations and Future Directions:

A limitation of this study was the use of established ovarian cancer cell lines, which may not fully represent the diversity of ovarian cancer cell lines or heterogeneity of ovarian cancer observed in patients. Future studies should therefore evaluate the optimized microfluidic platform using other HM and NM cell lines for ovarian cancer and patient-derived ovarian cancer cells to further investigate its physiological and translational relevance.

A further limitation was that the present study investigated cancer cell adhesion to P-selectin-coated microfluidic channels without incorporating human peritoneal mesothelial cells or other components of the peritoneal tumor microenvironment. Incorporating human peritoneal mesothelial cells and additional components of the peritoneal tumor microenvironment may further improve the physiological relevance of the model and enable investigation of tumor-mesothelial adhesion under more physiologically representative conditions.

In addition, the present study focused on optimization of P-selectin coating concentration and did not directly investigate the molecular mechanisms underlying the differential P-selectin-mediated adhesion observed between HM and NM cell lines. Future studies should therefore investigate the expression of P-selectin-binding molecules, including sialyl Lewis X and CD24, to further characterize the molecular basis of differential adhesion between ovarian cancer cell lines.

Therefore, future studies should focus on further optimizing the microfluidic chip for NM cells to improve the discrimination between HM and NM adhesion phenotypes, as well as on approaches to achieving high sensitivity and high specificity while minimizing the sensitivity-specificity trade-off.

In the future, the optimized platform may also provide a controlled system for evaluating factors or therapeutic interventions that alter P-selectin-mediated ovarian cancer cell adhesion under flow conditions.

Conclusion

This study investigated and optimized the P-selectin coating concentration for a microfluidic platform designed to study ovarian cancer cell adhesion under flow conditions. A P-selectin concentration of 25 μg/mL was selected as the optimal working concentration based on signal intensity, variance, and sensitivity and specificity results. The optimized platform demonstrated differential adhesion between HM Kuramochi and NM ovarian cancer cell lines, supporting its potential for investigating metastatic adhesion phenotypes. Further optimization for NM cells and validation using patient-derived ovarian cancer cells may improve the sensitivity, specificity, and translational relevance of the platform.

References

An, Y., & Yang, Q. (2021). Tumor-associated macrophage-targeted therapeutics in ovarian cancer. *International Journal of Cancer*, *149*(1), 21-30.

Carroll, M. J., Fogg, K. C., Patel, H. A., Krause, H. B., Mancha, A. S., Patankar, M. S., ... & Kreeger, P. K. (2018). Alternatively-activated macrophages upregulate mesothelial expression of P-selectin to enhance adhesion of ovarian cancer cells. *Cancer research*, *78*(13), 3560-3573.

Cortesi, M., Warton, K., & Ford, C. E. (2024). Beyond 2D cell cultures: how 3D models are changing the *in vitro* study of ovarian cancer and how to make the most of them. *PeerJ*, *12*, e17603. https://doi.org/10.7717/peerj.17603

Haley, J., Tomar, S., Pulliam, N., Xiong, S., Perkins, S. M., Karpf, A. R., Mitra, S., Nephew, K. P., & Mitra, A. K. (2016). Functional characterization of a panel of high-grade serous ovarian cancer cell lines as representative experimental models of the disease. *Oncotarget*, *7*(22), 32810–32820. https://doi.org/10.18632/oncotarget.9053

Hassan, A. A., Artemenko, M., Tang, M. K. S., & Wong, A. S. T. (2020). Selectins: An Important Family of Glycan-Binding Cell Adhesion Molecules in Ovarian Cancer. *Cancers*, *12*(8), 2238. https://doi.org/10.3390/cancers12082238

Ip, C., Li, SS., Tang, M. *et al.* Stemness and chemoresistance in epithelial ovarian carcinoma cells under shear stress. *Sci Rep* **6**, 26788 (2016). https://doi.org/10.1038/srep26788

Li, SS., Ip, C.K.M., Tang, M.Y.H. *et al.* Sialyl Lewis^{x}-P-selectin cascade mediates tumor–mesothelial adhesion in ascitic fluid shear flow. *Nat Commun* **10**, 2406 (2019). https://doi.org/10.1038/s41467-019-10334-6

Lim, S. Y., Aboelnasr, L. S., & El-Bahrawy, M. (2025). Tumour-on-Chip Models for the Study of Ovarian Cancer: Current Challenges and Future Prospects. *Cancers*, *17*(19), 3239. https://doi.org/10.3390/cancers17193239

Lopez, E., Kamboj, S., Chen, C., Wang, Z., Kellouche, S., Leroy-Dudal, J., Carreiras, F., Lambert, A., & Aimé, C. (2023). In Vitro Models of Ovarian Cancer: Bridging the Gap between Pathophysiology and Mechanistic Models. *Biomolecules*, *13*(1), 103. https://doi.org/10.3390/biom13010103

Mazidimoradi, A., Momenimovahed, Z., Allahqoli, L., Tiznobaik, A., Hajinasab, N., Salehiniya, H., & Alkatout, I. (2022). The global, regional and national epidemiology, incidence, mortality, and burden of ovarian cancer. *Health Science Reports*, *5*(6), e936.

Mitra, A. K., Davis, D. A., Tomar, S., Roy, L., Gurler, H., Xie, J., Lantvit, D. D., Cardenas, H., Fang, F., Liu, Y., Loughran, E., Yang, J., Sharon Stack, M., Emerson, R. E., Cowden Dahl, K. D., V Barbolina, M., Nephew, K. P., Matei, D., & Burdette, J. E. (2015). In vivo tumor growth of high-grade serous ovarian cancer cell lines. *Gynecologic oncology*, *138*(2), 372–377. https://doi.org/10.1016/j.ygyno.2015.05.040

Morikis, V. A., Baker, B., Martin, J. A., Schab, A., DiMauro, A., Longmore, G. D., & Grither, W. R. (2026). Ex vivo microfluidic model identifies a role for shear stress during ovarian tumor cell attachment to peritoneal mesothelial cells. *ACS Biomaterials Science & Engineering*, *12*(2), 1286.

Sadeghi, S. and Elitas, M. (2017). *A simple, bubble-free cell loading technique for culturing mammalian cells on lab-on-a-chip devices*. Chips and Tips, Royal Society of Chemistry, 28 February.

Wolters-Eisfeld, G., & Oliveira-Ferrer, L. (2024). Glycan diversity in ovarian cancer: Unraveling the immune interplay and therapeutic prospects. In *Seminars in Immunopathology* (Vol. 46, No. 6, p. 16). Berlin/Heidelberg: Springer Berlin Heidelberg.